analytical chemistry

Article

pubs.acs.org/ac

Label-Free Fluorescent Detection of Ions, Proteins, and Small Molecules Using Structure-Switching Aptamers, SYBR Gold, and Exonuclease I

Dongmei Zheng, Ruxing Zou, and Xinhui Lou*

Department of Chemistry, Capital Normal University, Xisanhuan North Rd. 105, Beijing, China, 100084

Supporting Information

ABSTRACT: We have demonstrated a label-free sensing strategy employing structure-switching aptamers (SSAs), SYBR Gold, and exonuclease I to detect a broad range of targets including inorganic ions, proteins, and small molecules. This nearly universal biosensor approach is based on the observation that SSAs at binding state with their targets, which fold into secondary structures such as quadruplex structure or Y shape structure, show more resistance to nuclease digestion than SSAs at unfolded states. The amount of aptamer left after nuclease reaction is proportional to the concentrations of the targets and in turn is proportional to the fluorescence intensities from SYBR Gold that can only stain nucleic acids but not their digestion products, nucleoside monophosphates (dNMPs). Fluorescent assays employing this mechanism for the detection of potassium ion (K^+) are sensitive, selective, and convenient. Twenty μM K^+ is readily detected even at the presence of a 500-fold excess of Na^+. Likewise, we have generalized the approach to the specific and convenient detection of proteins (thrombin) and small molecules (cocaine). The assays were then validated by detecting K^+, cocaine, and thrombin in urine and serum or cutting and masking adulterants with good agreements with the true values. Compared to other reported approaches, most limited to G-quadruplex structures, the demonstrated method has less structure requirements of both the SSAs and their complexes with targets, therefore rending its wilder applications for various targets. The detection scheme could be easily modified and extended to detection platforms to further improve the detection sensitivity or for other applications as well as being useful in high-throughput and paralleled analysis of multiple targets.

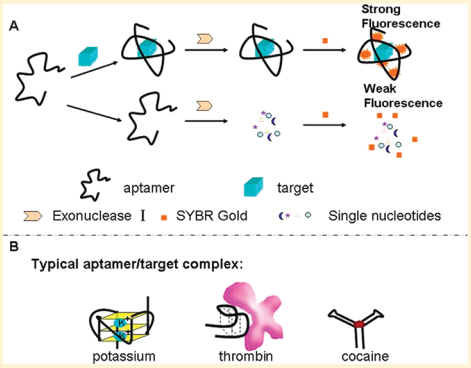

Nucleic acid-based aptamers[1−3] can be selected in vitro against a wide range of targets including low-molecule-weight substrates, macromolecules such as proteins,[2] or cell surface,[3] and for a wide range of applications including diagnostics, molecules imaging, targeted therapeutics, gene delivery, and drug delivery.[4,5] Unlike most conventional affinity reagents (e.g., antibodies), a group of aptamers called structure-switching aptamers (SSAs)[6] can undergo target-induced conformational change, which is actually the basis of many sensing approaches including fluorescent methods, colorimetric methods,[7,8] and electrochemical methods.[9,10]

Biosensing by fluorescence is one of the most popular methods for the design of aptamer-based assays, largely because of the ease of detection, good sensitivity, and potential for high-throughput analysis. However, many of the existing methods require labeling of the aptamers with fluorophores (and quenchers)[11−15] or utilizing modified bases,[16] which is expensive and time-consuming. Furthermore, aptamer labeling with different fluorescent and quenching molecules can even influence the properties of the target binding aptamers.[17] These drawbacks have inspired the efforts to develop label-free methods for fluorescent detection. Several label-free methods have been reported to sensitively detect the targets by utilizing conjugated polymers[8,18] or DNA structure selective fluorescent dyes,[17,19−21] fluorescent dyes to report conformational change of aptamers upon recognition of given targets. Those methods are in general quite simple, sensitive, and selective. However, these types of methods usually require the extensive optimization of oligonucleotide sequences in order to control the binding sites between the dyes and DNA, which limits the generalization of the methods for other targets. For example, the fluorescent sensing basis of cationic conjugated polymers is the direct dependence of fluorescence intensity on the conformational change of the polymer that would wrap the folded aptamer. That is to say, the conformation of the polymer highly relies on the structure of the folded aptamer. For this reason, the polymer-based method may not work well for the aptamer with partially formed secondary structures (such as cocaine aptamer) at the absence of targets. Cekan reported that both the EPR and the fluorescence data for anticocaine aptamer indicated that two helix structures were already formed before cocaine binding,[22] which resulted in the insufficient conformational changes to be reported by conjugated polymers. The G-quadruplex structure selective fluorescent dye-based methods

Received: November 30, 2011
Accepted: March 16, 2012
Published: March 16, 2012

Table 1. Probes Used in This Study

name	sequences (5′---3′)	description
probe 1	TGAGGGTGGGGAGGGTGGGGAA	antipotassium aptamer
probe 2	AGTCCGTGGTAGGGCAGGTTGGGGTGACT	antithrombin aptamer
probe 3	CAGGCTACGGCACGTAGAGCATCACCATGATCCTG	random sequence used for thrombin selectivity test
probe 4	GGGAGTCAAGAACAAAGTTCTTCAATGAAGTGTGGGACGACA	anticocaine aptamer
probe 5	ACCTGGGGGAGTATTGCGGAGGAAGGTCTGTA	random sequence used for cocaine selectivity test

have limited applications for the aptamer−target complexes with non-G-quadruplex structures. In addition, the signaling molecules, conjugated polymers, or structure selective fluorescent dyes are not commercially available and have to be synthesized, which certainly limits the applications of those methods. Therefore, it is highly desirable to develop a general, label-free, and synthesis-free approach for the facile detection of non-nucleic acid targets with less structure requirements of both the SSAs and their complexes with targets.

Nucleases are specific enzymes capable of cleaving the phosphodiester bonds between nucleotides of nucleic acids either from the ends or internally. These enzymes, such as flap nuclease,[23] nicking enzymes,[24−26] S1 nuclease,[27−29] Exo III,[30−32] Exo I,[33−35] and so on, are widely used in various biosensing techniques to achieve exceptional detection selectivity and sensitivity for DNA detection. Recently, the application of nucleases in biosensing has extended to non-nucleic acid targets by utilizing SSAs as recognition molecules.[36−42] Specifically, Exo I has been used for protein detection.[37,43] For example, Wang et al. have demonstrated a sensitive method for thrombin detection by combining PCR amplification with the retarded Exo I digestion of the G-quadruplex formed at the presence of thrombin.[37] However, the demonstrated methods were only applied to the SSAs that can fold into G-quadruplex structures. In order to further exploit the applicability of Exo I in the detection of non-nucleic acid targets, we recently developed a microfluidic method for sensitive Hg^{2+} detection by taking advantage of the selective digestion capability of Exo I, in which hairpin-like double-stranded DNAs (dsDNA) formed due to the coordination of T-Hg^{2+}-T are more difficult to be digested by Exo I than the random coil ssDNA.[44]

Inspired and encouraged by the exceptional structure selectivity of Exo I, here for the first time, we report on a nearly "universal" fluorescent Exo I-based assay for the detection of small-molecules, proteins, and inorganic ions that relies on the conformational changes of SSAs. We demonstrate that the resistance of Exo I digestion is applied not only for G-quadruplex structures and hairpin structures but also for other structures. Our method employs SYBR Gold, one of the most popular used commercial dyes for nucleic acid stain, and Exo I, one of the cheapest nucleases for structure-selective digestion of folded and unfolded SSAs. Such a general method offers several advantages over existing techniques such as commercial availability, low cost, high specificity, and potential for high-throughput parallel analysis.

EXPERIMENTAL SECTION

Materials. All the oligonucleotide sequences used in this study were synthesized and purified through HPLC by Sangon Biotechnology Co., Ltd. (Shanghai, China), and sequence information was list in Table 1. The fluorescent dye SYBR Gold (10 000× concentrated) was purchased from Invitrogen (CA, USA). Exo I was bought from TaKaRa Biotechnology Inc. (Dalian, China). Thrombin and bovine serum albumin (BSA) were bought from Sigma (St. Louis, MO). Cocaine, ecogonine methyl ester (EME), and benzoyl ecgonine (BE) were bought from State Food and Drug Administration (Beijing, China). All other reagents were of analytical grade and bought from AccuStandard (Beijing, China).

Fluorescent Detection of K^+. The K^+ aptamer (probe 1, Table 1) solutions were heated at 90 °C for 5 min and gradually cooled to the room temperature. Ten μL of aptamer solution (10 μM) was mixed with 969 μL of 1× potassium binding buffer (50 mM Tris-HCl, 2 mM $MgCl_2$, pH 8.3) containing different concentrations of K^+ in tubes. Samples were incubated at room temperature for a certain period of time as indicated in the figure captions or the main text. Then, 5U of Exo I was added to the sample tubes and incubated at 37 °C for 40 min (or 10 min). Subsequently, 20 μL of 10× SYBR Gold was mixed with the samples, and the fluorescent intensities were recorded using a F-4500 fluorescence spectrophotometer (Shanghai Hitachi). The assay procedures for ammonium (NH_4Cl), lithium (LiCl), sodium (NaCl), calcium ($CaCl_2$), and magnesium ($MgCl_2$) ions were the same as those for K^+ ions.

Fluorescent Detection of Thrombin. All assay conditions were the same as those used for the detection of K^+, except that the K^+ aptamer was replaced by antithrombin aptamer (probe 2, Table 1) and the binding buffer was 1× thrombin binding buffer (100 mM Tris, 140 mM NaCl, 20 mM $MgCl_2$, 20 mM KCl). In addition, samples were incubated at room temperature for 1 h to ensure the binding of the thrombin with its aptamer, and 2.5 U of Exo I was added into the sample tubes and incubated at room temperature for 30 min. Subsequently, 10 μL of 100× SYBR Gold was mixed with the samples, and the fluorescent intensities were then recorded as above.

Fluorescent Detection of Cocaine. All assay conditions were the same as those used for the detection of K^+, except that the K^+ aptamer was replaced by anticocaine aptamer and the binding buffer was 1× cocaine binding buffer (25 mM Tris-HCl, 0.15 M NaCl, 2 mM $MgCl_2$, pH 8.0). In addition, samples were incubated at room temperature for 1 h to ensure the binding of the cocaine with its aptamer, and 5 U of Exo I was added into the sample tubes and incubated at 37 °C for 30 min.

Application. Both urine and serum samples were used to confirm the feasibility of this sensor for analysis of real-world samples. Urine samples were harvested from two members of our laboratory, filtered through 0.22 μM membranes and directly used in cocaine detections. The serum samples were obtained from the hospital and directly used in cocaine and thrombin detections. Specifically, the urine samples (or serum samples) were diluted 100-fold with 1× binding buffer containing 250 μM cocaine (or 680 nM thrombin) and followed by other steps as described above. For K^+ detection, the harvested urine samples were extracted three times by methylene dichloride (volume ratio/sample/methylene dichloride = 3:1) and diluted 250-fold with 1× potassium

dx.doi.org/10.1021/ac300690r | Anal. Chem. 2012, 84, 3554−3560

binding buffer. The serum samples were filtered through the NAP-5 column and then diluted 20 times with 1× binding buffer. Both samples were subsequently analyzed as described above (1 h incubation with aptamer at room temperature and 40 min Exo I reaction at 37 °C).

The cocaine sensor was also validated with adulerated samples (sugar, flour, baking soda, and pepper). Each of them were mixed with cocaine at 1:1 or 10:1 mass ratios.

RESULTS AND DISCUSSION

Structure-switching aptamers (SSAs) have attracted tremendous attention in the biosensing field due to their unique property: significant conformational changes happen when binding with their targets. For different targets, the resulting conformational structures vary significantly. As demonstrated in Scheme 1, the K^+ aptamer folds into a G-quadruplex structure

Scheme 1. Label-Free Fluorescent Assays for Detection of Potassium, Thrombin, and Cocaine Using Structure-Switching Aptamers, SYBR Gold, and Exo I

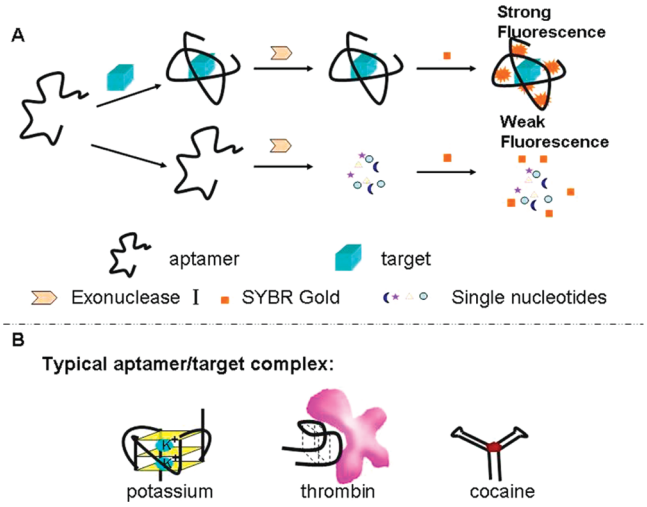

in the presence of K^+, and K^+ was trapped inside the G-quadruplex pocket;[20,45] antithrombin aptamer also folds into G-quadruplex structure at the presence of thrombin. The G-quadruplex is half-surrounded by thrombin;[46] and the cocaine aptamer folds into a Y shape and encapsulates cocaine in the intersection.[11,12] Even though the structures of the aptamer–target complexes vary, those structures are all obviously different from the random coil structure of single stranded DNAs. Therefore, it is highly possible that all those structures would have stronger resistance to the digestion of single strand specific nucleases. On the basis of this assumption, we develop a label-free fluorescent assay for the detection of a wide range of targets including inorganic ions, proteins, and small molecules using SSAs, SYBR Gold, and Exo I (Scheme 1). In this method, the presence of the targets causes the conformational changes of the SSAs and the formation of the aptamer–target complexes. Then, Exo I is added into the mixture to selectively digest the unfolded aptamers which are the preferred substrates of Exo I. Finally, SYBR Gold is introduced to insert into the aptamer–target complexes and results in the significantly increased fluorescent intensities, which is directly proportional to the concentrations of the targets.

In this assay, SYBR Gold was chosen as the fluorescent dye due to its commercial availability, low toxicity, good stability, excellent sensitivity, and specificity for nucleic acids.[47,48] Exo I was chosen as the structure selective nuclease due to its good selectivity, low price, and importantly buffer compatibility for both aptamer–target binding and nuclease digestion.

To prove the feasibility of the proposed method, we started with the detection of K^+. It is well-known that K^+ plays an important role in living organisms, such as reducing the risk of high blood pressure and stoke, maintaining muscular strength, balancing the pH, etc.[49] Besides, an unbalance of K^+ ions is associated with several diseases.[50] Therefore, monitoring of K^+ becomes an increasing demand. To meet this goal, a number of highly sensitive and selective fluorescent K^+ sensors utilizing gold nanoparticles,[7,51] DNAzymes,[52,53] polymer materials,[18,54,55] and fluorophores[50,56,57] have been developed, on the basis of the formation of G-quadruplex structure at the presence of K^+. Despite the success in the development of K^+ detection sensors, most of the reported architectures suffer from low sensitivity (Table 2). Here, we demonstrated the sensitive detection of K^+ using K^+ aptamer (probe 1, Table 1), SYBR Gold, and Exo I. In the absence of K^+, probe 1 is in the random coil state, and Exo I can completely degrade this single strand into nucleotides. Upon addition of K^+, the aptamer is able to be folded into a G-quadruplex structure (Scheme 1) and be protected from the degradation by Exo I; after staining by SYBR Gold, a strong fluorescence is produced.

As shown in Figure 1A, without nuclease digestion involved, the sample with or without K^+ (1 mM) exhibited similar fluorescent intensities; only a slight red-shift of the emission band of SYBR Gold from 540 ± 2 nm to 542 ± 1 nm was observed in the presence of K^+. In contrast, when Exo I digestion was included in the assay steps, just as we expected, the sample with 1 mM K^+ showed a dramatically higher fluorescent intensity than the blank sample due to the stronger resistance of the G-quadruplex structure formed by probe 1 and K^+ to nuclease digestion (Figure 1B), which was further confirmed by the PAGE gel electrophoresis (Figure S-1, Supporting Information). In addition, the fluorescence peaks from SYBR Gold shifted to 544 ± 1 nm. Interestingly, we did not observe the same phenomenon for cocaine and thrombin

Table 2. Comparison of Aptamer-Based Sensors for Potassium Detection

detection method	strategy	detection limit	existing problems
colorimetric[51]	aggregation of unmodified AuNPs	1 mM	not applicable for colored samples
colorimetric[7]	aggregation of AuNPs assembled with thiolated DNA aptamers	100 μM	cumbersome preparation of coated AuNPs
electrochemistry[10]	electron transfer	15 μM	cumbersome assembly of the thiolated electrode
fluorescence[14]	FRET and cationic conjugated polyelectrolyte	1.5 nM	dual-labeled oligos
fluorescence[18]	external stimuli sensitive polymer	100 μM	cumbersome preparation of polymer microarray
fluorescence[19]	parallel G-quadruplex specific fluorescent dye	0.5 mM	not applicable for nonparallel G-quadruplex
fluorescence[17]	ds DNA specific dye, heating 70 °C	0.05 μM	not applicable for thermo labile samples

dx.doi.org/10.1021/ac300690r | Anal. Chem. 2012, 84, 3554–3560

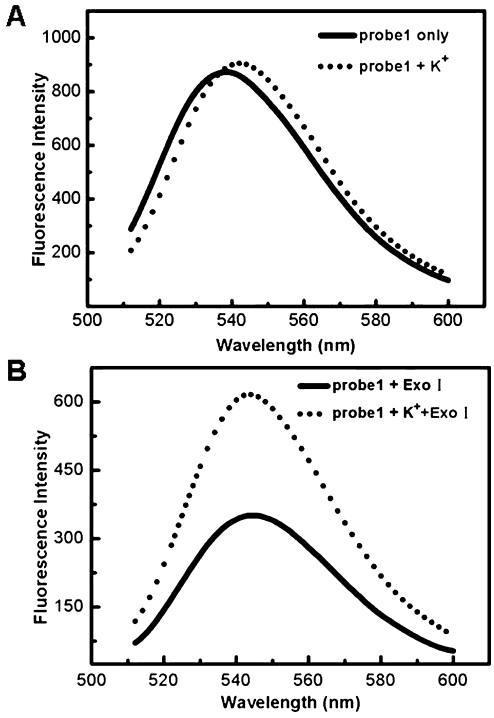

Figure 1. The fluorescence spectra of SYBR Gold/probe 1 mixture with or without 1 mM K^+, without (A) or with (B) the Exo I digestion involved.

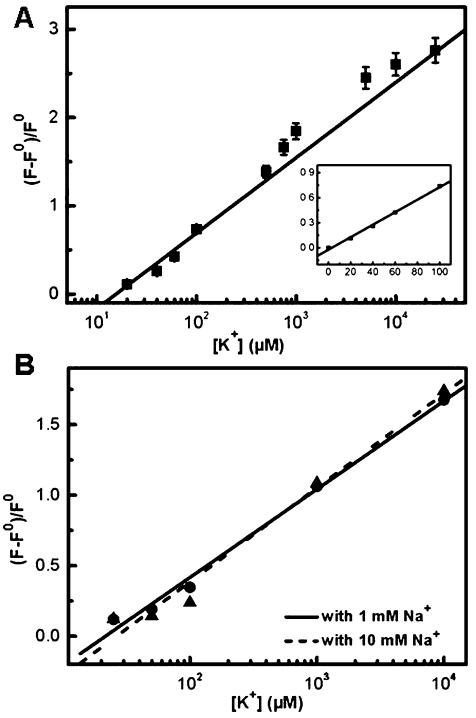

Figure 2. Relative fluorescence intensities $(F - F^0)/F^0$ of the SYBR Gold/probe 1 mixture upon addition of different concentrations of K^+ without Na^+ (A) or with 1 mM (solid line) or 10 mM (dash line) Na^+ (B). F^0 and F stand for the fluorescent intensity in the absence and presence of potassium ions.

detection (The peaks were all at 541 ± 1 nm). These red-shifts of peaks from SYBR Gold at the presence of K^+ and Exo I are quite unique, which might result from the energy level changes of SYBR Gold due to its conformational changes under different conditions. Please note that the differences of the fluorescence intensities in Figure 1A,B are due to the fact that both the blank sample and the K^+ containing sample all undergo Exo I digestion, which can be minimized under optimized conditions to decrease the digestion of the blank sample.

The assay turned out to be quite sensitive, as shown in Figure 2A, as low as 20 μM K^+ was able to be detected with a dynamic range more than 3 orders of magnitude. Especially, a fairly well linear response was observed with the correlation efficiencies of 0.979 and 0.998 for the whole detection range and for the low micromolar concentrations of K^+ (inset in Figure 2A), respectively. This sensitivity should be able to be further improved by optimizing conditions such as the concentration of SYBR Gold, enzymatic reaction time, and so on.

Assay time is a critical parameter to consider for practical applications. With the purpose of decreasing the assay time, we studied four different assay conditions with significantly shortened incubation times and Exo I reaction times (Table S-1, Supporting Information). Under all conditions, 100 μM K^+ was still able to be clearly detected. The lowest $(F - F^0)/F^0$ value (0.41) was achieved by modified assay 1 (incubation time, 1 h; Exo I reaction time, 40 min). Even under this assay condition, K^+ was still able to be detected with a little bit lower correlation efficiency of 0.954 for both the whole detection range and for the low micromolar concentrations of K^+ with a detection limit of 20 μM (Figure S-2, Supporting Information). Among the tested assay conditions, the shortest whole assay time was 25 min (modified assay 4). The assay time could be further decreased by optimizing enzymatic reactions. This assay time is comparable to other reported methods.[7,19,20]

K^+ under extracellular conditions coexists with Na^+ ions. Typically, in blood, the concentration of K^+ is 3.5−5.3 mM, whereas that of Na^+ is 135−148 mM.[58] The interference of Na^+ is one of the major problems to limit the applications of lots of sensors in the real world (Table 2).[59] In order to test how well our sensor could stand the interference of Na^+, we repeated the sensitivity test experiment as we show in Figure 2A, except adding 1 mM and 10 mM Na^+ into each assay, respectively. As shown in Figure 2B, the presence of 1 mM or 10 mM Na^+ did not interfere with the detection of K^+, and 20 μM K^+ was still able to be detected at the presence of a 500-fold excess of Na^+. To test the specificity of the sensor, the possible interference of some other common ions (e.g., Li^+, NH_4^+, Ca^{2+}, Mg^{2+}) were evaluated. As shown in Figure 3, Li^+, NH_4^+, and Mg^{2+} could not trigger the folding of probe 1 into a G-quadruplex structure to resist Exo I digestion, and thus, the fluorescence intensities were similar to that of the blank sample. Ca^{2+} caused about a 20% increase of the fluorescence intensity compared to the blank sample, while K^+ at the same concentration (1 mM) brought about a 150% increase. It is worth pointing out that, in the physiological condition, the concentrations of Ca^{2+} and Mg^{2+} are in the same order as that of K^+: 3.04−5.27 mM Ca^{2+} and 1.01−2.12 mM Mg^{2+}.[60] Thus, the presence of Ca^{2+} and Mg^{2+} should not interfere with the detection of K^+ under physiological conditions. In contrast, Na^+ resulted in about a 15% decrease of fluorescence intensity compared to the blank sample. The main reason could be that Na^+ could slightly enhance the activity of Exo I. On the other hand, the higher amount of Na^+ can also trigger the formation of G-quadruplex structure,[19] which would increase the resistance to Exo I

dx.doi.org/10.1021/ac300690r | Anal. Chem. 2012, 84, 3554−3560

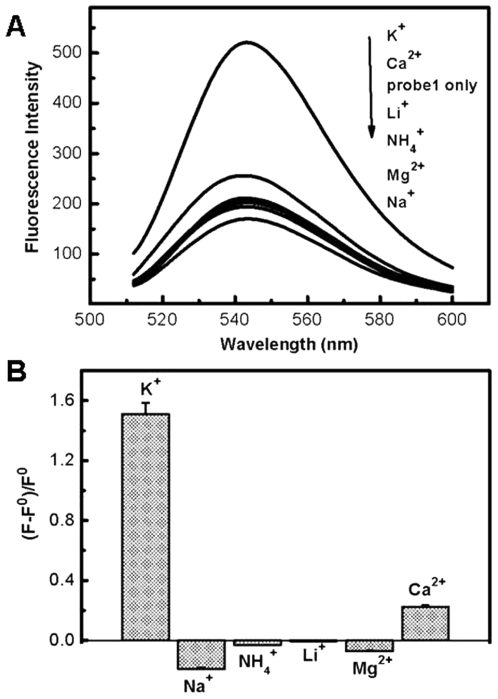

Figure 3. (A) The fluorescence spectra from solutions containing probe 1, SYBR Gold, Exo I, and 1 mM metal ions. (B) The dependence of relative fluorescence intensities $(F - F^0)/F^0$ on the various ions. F^0 and F stand for the fluorescence intensity in the absence and presence of metal ions. Experimental conditions are the same as those used for K^+ detection.

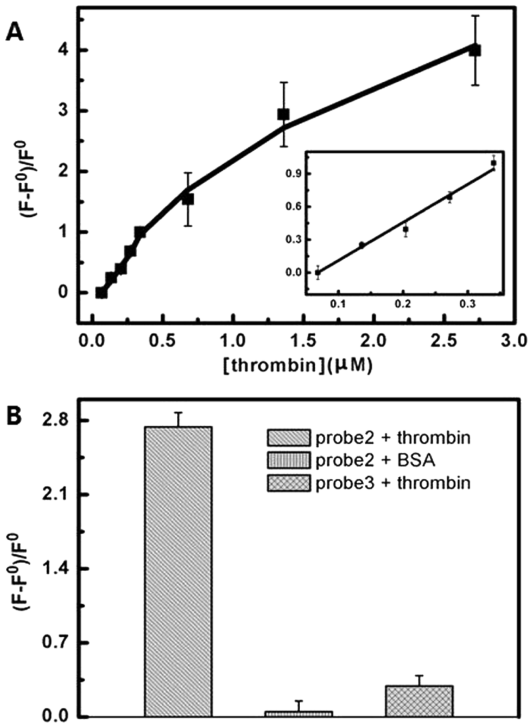

Figure 4. General applicability of the detection strategy for thrombin detection: (A) Relative fluorescence intensities $(F - F^0)/F^0$ of the SYBR Gold/probe 2 mixture upon addition of different concentrations of thrombin. (B) The dependence of relative fluorescence intensities $(F - F^0)/ F^0$ on the various targets (thrombin or BSA) or probes (probe 2 or probe 3). F^0 and F stand for the fluorescence intensity in the absence and presence of targets.

reaction. Thanks to the opposite effects, the interference from Na^+ was minimized. As demonstrated in Figure 2B, 20 μM K^+ was still able to be detected in the presence of a 500-fold excess of Na^+.

To exploit the broader applicability of our approach, we modified the assay for thrombin detection using Bock's thrombin-binding aptamer (probe 2, Table 1),[46] which also folds from a single-stranded state to a largely G-quadruplex structure upon target binding. Similarly, we employed control (aptamer only) and test (aptamer plus thrombin) solutions. As shown in Figure S-3 (Supporting Information), without nuclease digestion involved, the sample with or without thrombin (1 μM) exhibited similar fluorescent intensities. In sharp contrast, after Exo I digestion, the sample with 1 μM thrombin showed a dramatically higher fluorescence intensity than the control sample due to the stronger resistance of the G-quadruplex structure formed by thrombin-binding aptamer and thrombin. Under nonoptimized conditions, the assay showed a wide dynamic range, and a fairly well linear response was observed at the nanomolar concentrations of thrombin (R^2 = 0.96, inset in Figure 4A). Importantly, the assay was quite selective, no such fluorescence protection phenomenon was observed either by replacing thrombin by other proteins, like BSA, or replacing the thrombin-binding aptamer with random ssDNA (probe 3, Table 1) (Figure 4B, Figure S-4, Supporting Information).

As demonstrated above, our assay worked very well for both ions and proteins. However, in these two examples, the aptamer–target complexes all have the G-quadruplex structures. It would be very interesting to see if our assay can also be applied for other targets that can trigger the formation of aptamer–target complexes with different structures. The assay was then applied to the detection of cocaine under the similar conditions as used for K^+ and thrombin detection. It has been well studied that the anticocaine aptamer can fold into Y shape structure with cocaine.[12] Similarly, as shown in Figure S-5, without nuclease digestion involved, the sample with or without cocaine (500 μM) exhibited the same fluorescence intensities. In sharp contrast, after Exo I digestion, the sample with cocaine showed a dramatically higher fluorescence intensity than the control sample due to the stronger resistance of the Y shape structure formed by cocaine-binding aptamer and cocaine. Under nonoptimized conditions, the assay had the calculated detection limit (S/N = 3) of 5 μM, which is comparable with some other labeled fluorescent methods (Figure 5A).[11,12] Importantly, the assay was quite selective; no such fluorescence protection phenomenon was observed either by replacing cocaine by its analogues, like BE and EME, or replacing the anticocaine aptamer with random ssDNA (probe 5, Table 1) (Figure 5B, Figure S-6, Supporting Information).

To assess the assay's ability to detect targets in complex, tainted samples, we tested sensors for their ability to detect cocaine, thrombin, and K^+ in the presence of biological fluids and other contaminants, repectively. Specifically, we find that the assay readily detected 500 μM cocaine in human urine or serum, with $(F - F^0)/F^0$ values of 1.6 and 1.5, respectively, which all agree with the value of the strandard cocaine sample (Table 3). Similarly, the assay is also effectively impervious to the many agents employed to cut or mask cocaine including sugar, flour, baking soda, and pepper. We also successfully detected 680 nM thrombin spiked in the human serum with less than 7% lower fluorescence intensity compared to the

dx.doi.org/10.1021/ac300690r | Anal. Chem. 2012, 84, 3554–3560

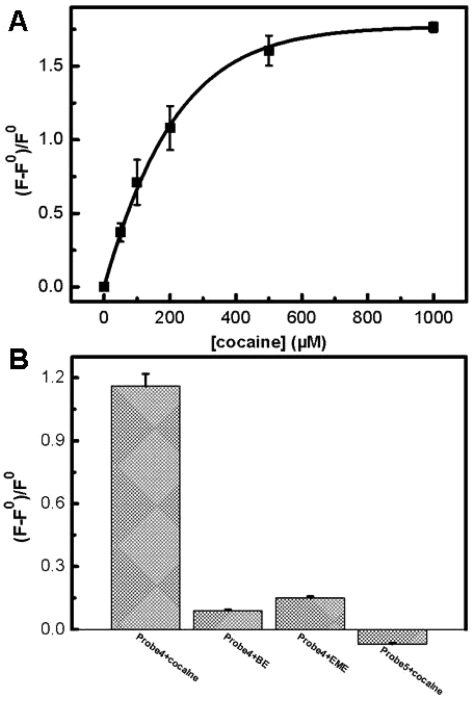

Figure 5. General applicability of the detection strategy for cocaine detection: (A) Relative fluorescence intensities $(F - F^0)/F^0$ of the SYBR Gold/probe 4 mixture upon addition of different concentrations of cocaine. (B) The dependence of relative fluorescence intensities $(F - F^0)/F^0$ on the various targets (cocaine or BE or EME) or probes (probe 4 or probe 5). F^0 and F stand for the fluorescence intensity in the absence and presence of targets.

Table 3. Cocaine Detection in Adulterants[a]

adulterant	$(F - F^0)/F^0$
none	1.6
equal mass sugar	1.6
equal mass baking soda	1.6
equal mass flour	1.3
equal mass pepper	1.4
10× mass sugar	1.6
urine	1.6
serum	1.5

[a]The detailed experimental conditions were described in the Experimental Section.

standard thrombin sample in buffer (Figure S-7, Supporting Information). The level of K^+ in serum and urine is one of the important values for disease diagnostics and has to be in the right range (3.5−5.5 mM for serum and 25−125 mmol per day for urine) to maintain healthy. We then detected the K^+ in real urine and serum samples with moderate success. As shown in Table 4, the concentrations of K^+ in real urine and serum samples measured by our method are averagely 84 ± 8% of the values measured by ICPMS. Those relatively lower values could be due to the different sample pretreatment methods used for these two methods. For ICPMS measurements, microwave digestions, one of the most efficient sample pretreatment methods, were conducted before injection. However, for our method, the simple filtration (for serum sample) or extraction (for urine sample) was performed before performing the assay, which is a desired simple sample treatment method for practical use. Even though the values achieved by our assays are a little bit lower than the standard ICPMS method, it is still attractive considering its simple and fast operation procedure.

Table 4. Potassium Detection in Real Samples

sample	ICPMS (mM)	content (mM)	ratio
urine 1	13.2	12.3	93%
urine 2	21.6	16.3	76%
serum 1	4.9	3.8	78%
serum 2	6.1	5.4	89%

CONCLUSIONS

In summary, we have demonstrated a general sensing strategy employing structure-switching aptamers (SSAs), SYBR Gold, and Exo I to detect a broad range of targets including inorganic ions, proteins, and small molecules. This nearly universal biosensor approach is based on the observation that SSAs at a binding state with their targets, which fold into secondary structures such as quadruplex structure or Y shape structure, show more resistance to nuclease digestion than SSAs at unfolded states. Compared with other assays, our method has characteristics: (1) it is a label-free method, which eliminates the need for modification of the DNA and greatly reduces the cost; (2) the elements, used in the assays, are cheap and commercially available; (3) the assay is highly sensitive for K^+ detection, even in the presence of a 500-fold excess of Na^+; and (4) importantly, it is a nearly universal method due to the exceptional structure selectivity of Exo I. The principle can be extended to the detection of other targets, like ions, small molecules, and proteins. It can be foreseen that the simple approach demonstrated here could be modified and coupled with other various detection platforms as well as being useful in high-throughput and paralleled analysis of multiple targets.

ASSOCIATED CONTENT

Supporting Information

Additional information as noted in text. This material is available free of charge via the Internet at http://pubs.acs.org.

AUTHOR INFORMATION

Corresponding Author

*E-mail: xlou9999@yahoo.com. Tel: +86-10-68902491 ext. 808. Fax: +86-10-68902320.

Notes

The authors declare no competing financial interest.

ACKNOWLEDGMENTS

D.M., R.Z., and X.L. contributed equally to this work. This work was supported by National Natural Science Foundation (20975108), Shanghai Pujiang Program (09PJ1411800), and Funding Project for Academic Human Resources Development in Institutions of Higher Learning under the Jurisdiction of the Beijing Municipality (PHR20100718).

REFERENCES

(1) Osborne, S. E.; Ellington, A. D. *Chem. Rev.* **1997**, *97*, 349−370.
(2) Lou, X. H.; Qian, J. R.; Xiao, Y.; Viel, L.; Gerdon, A. E.; Lagally, E. T.; Atzberger, P.; Tarasow, T. M.; Heeger, A. J.; Soh, H. T. *Proc. Natl. Acad. Sci. U. S. A.* **2009**, *106*, 2989−2994.
(3) Sefah, K.; Shangguan, D.; Xiong, X. L.; O'Donoghue, M. B.; Tan, W. H. *Nat. Protoc.* **2010**, *5*, 1169−1185.
(4) Tan, W.; Wang, H.; Chen, Y.; Zhang, X.; Zhu, H.; Yang, C.; Yang, R.; Liu, C. *Trends Biotechnol.* **2011**, *29*, 634−640.

(5) Famulok, M.; Mayer, G. *Acc. Chem. Res.* **2011**, *44*, 1349−1358.
(6) Vallee-Belisle, A.; Plaxco, K. W. *Curr. Opin. Struct. Biol.* **2010**, *20*, 518−526.
(7) Zhu, X. L.; Zhao, J.; Wu, Y.; Shen, Z. M.; Li, G. X. *Anal. Chem.* **2011**, *83*, 4085−4089.
(8) Ho, H. A.; Leclerc, M. *J. Am. Chem. Soc.* **2004**, *126*, 1384−1387.
(9) Li, D.; Song, S. P.; Fan, C. H. *Acc. Chem. Res.* **2010**, *43*, 631−641.
(10) Wu, Z. S.; Chen, C. R.; Shen, G. L.; Yu, R. Q. *Biomaterials* **2008**, *29*, 2689−2696.
(11) Stojanovic, M. N.; de Prada, P.; Landry, D. W. *J. Am. Chem. Soc.* **2001**, *123*, 4928−4931.
(12) Stojanovic, M. N.; de Prada, P.; Landry, D. W. *J. Am. Chem. Soc.* **2000**, *122*, 11547−11548.
(13) Tang, Z. W.; Mallikaratchy, P.; Yang, R. H.; Kim, Y. M.; Zhu, Z.; Wang, H.; Tan, W. H. *J. Am. Chem. Soc.* **2008**, *130*, 11268−11269.
(14) Kim, B.; Jung, I. H.; Kang, M.; Shim, H. K.; Woo, H. Y. *J. Am. Chem. Soc.* **2012**, *134*, 3133−3138.
(15) Zhang, J.; Wang, L.; Zhang, H.; Boey, F.; Song, S.; Fan, C. *Small* **2010**, *6*, 201−204.
(16) Hasegawa, T.; Hagihara, M.; Fukuda, M.; Nakano, S.; Fujieda, N.; Morii, T. *J. Am. Chem. Soc.* **2008**, *130*, 8804−8812.
(17) Choi, M. S.; Yoon, M.; Baeg, J.-O.; Kim, J. *Chem. Commun.* **2009**, 7419−7421.
(18) Lee, J.; Kim, H. J.; Kim, J. *J. Am. Chem. Soc.* **2008**, *130*, 5010−5011.
(19) Li, T.; Wang, E. K.; Dong, S. J. *Anal. Chem.* **2010**, *82*, 7576−7580.
(20) Qin, H. X.; Ren, J. T.; Wang, J. H.; Luedtke, N. W.; Wang, E. K. *Anal. Chem.* **2010**, *82*, 8356−8360.
(21) Huang, C.; Chang, H. *Chem. Commun.* **2008**, 1461−1463.
(22) Cekan, P.; Jonsson, E. O.; Sigurdsson, S. T. *Nucleic Acids Res.* **2009**, *37*, 3990−3995.
(23) Hall, J. G.; Eis, P. S.; Law, S. M.; Reynaldo, L. P.; Prudent, J. R.; Marshall, D. J.; Allawi, H. T.; Mast, A. L.; Dahlberg, J. E.; Kwiatkowski, R. W.; de Arruda, M.; Neri, B. P.; Lyamichev, V. I. *Proc. Natl. Acad. Sci. U. S. A.* **2000**, *97*, 8272−8277.
(24) Nakayama, S.; Yan, L.; Sintim, H. O. *J. Am. Chem. Soc.* **2008**, *130*, 12560−12561.
(25) Kiesling, T.; Cox, K.; Davidson, E. A.; Dretchen, K.; Grater, G.; Hibbard, S.; Lasken, R. S.; Leshin, J.; Skowronski, E.; Danielsen, M. *Nucleic. Acids. Res.* **2007**, *35*, e117.
(26) Li, J. J.; Chu, Y.; Lee, B. Y.-H.; Xie, X. S. *Nucleic. Acids. Res.* **2008**, *36*, e36.
(27) Kwon, D.; Kim, K.; Kwak, J. *Electroanalysis* **2008**, *20*, 1204−1208.
(28) Murakami, T.; Sumaoka, J.; Komiyama, M. *Nucleic. Acids. Res.* **2009**, *37*, e19.
(29) Liu, M. Y.; Yuan, M.; Lou, X. H.; Mao, H. J.; Zheng, D. M.; Zou, R. X.; Zou, N. L.; Tang, X. R.; Zhao, J. L. *Biosens. Bioelectron.* **2011**, *26*, 4294−4300.
(30) Lee, H. J.; Li, Y.; Wark, A. W.; Corn, R. M. *Anal. Chem.* **2005**, *77*, 5096−5100.
(31) Zuo, X. L.; Xia, F.; Xiao, Y.; Plaxco, K. W. *J. Am. Chem. Soc.* **2010**, *132*, 1816−1818.
(32) Freeman, R.; Liu, X.; Willner, I. *Nano Lett.* **2011**, *11*, 4456−4461.
(33) Davis, L. M.; Fairfield, F. R.; Harger, C. A.; Jett, J. H.; Keller, R. A.; Hahn, J. H.; Krakowski, L. A.; Marrone, B. L.; Martin, J. C.; Nutter, H. L.; Ratliff, R. L.; Shera, E. B.; Simpson, D. J.; Soper, S. A. *Genet. Anal. Biomol. Eng.* **1991**, *8*, 1−7.
(34) Werner, J. H.; Cai, H.; Jett, J. H.; Reha-Krantz, L.; Keller, R. A.; Goodwin, P. M. *J. Biotechnol.* **2003**, *102*, 1−14.
(35) Tran, H. T.; Gordenin, D. A.; Resnick, M. A. *Mol. Cell. Biol.* **1999**, *19*, 2000−2007.
(36) Juskowiak, B. *Anal. Bioanal. Chem.* **2011**, *399*, 3157−3176.
(37) Wang, X. L.; Li, F.; Su, Y. H.; Sun, X.; Li, X. B.; Schluesener, H. J.; Tang, F.; Xu, S. Q. *Anal. Chem.* **2004**, *76*, 5605−5610.
(38) Li, D.; Wieckowska, A.; Willner, I. *Angew. Chem., Int. Ed.* **2008**, *47*, 3927−3931.
(39) Lee, J. H.; Wang, Z. D.; Liu, J. W.; Lu, Y. *J. Am. Chem. Soc.* **2008**, *130*, 14217−14226.
(40) Liu, J. W.; Lu, Y. *J. Am. Chem. Soc.* **2004**, *126*, 12298−12305.
(41) Mor-Piperberg, G.; Tel-Vered, R.; Elbaz, J.; Willner, I. *J. Am. Chem. Soc.* **2010**, *132*, 6878−6879.
(42) Wu, D.; Z., Q.; Chu, X.; Wang, H.; Shen, G.; Yu, R. *Biosens. Bioelectron.* **2010**, *25*, 1025−1031.
(43) Wu, Z.; Zhen, Z.; Jiang, J. H.; Shen, G. L.; Yu, R. Q. *J. Am. Chem. Soc.* **2009**, *131*, 12325−12332.
(44) Yuan, M.; Zhu, Y. G.; Lou, X. H.; Chen, C.; Wei, G.; Lan, M. B.; Zhao, J. L. *Biosens. Bioelectron.* **2012**, *31*, 330−336.
(45) Brooks, T. A.; Kendrick, S.; Hurley, L. *FEBS J.* **2010**, *277*, 3459−3469.
(46) Bock, L. C.; Griffin, L. C.; Latham, J. A.; Vermaas, E. H.; Toole, J. J. *Nature* **1992**, *355*, 564−566.
(47) Chen, F.; Lu, J. R.; Binder, B. J.; Liu, Y. C.; Hodson, R. E. *Appl. Environ. Microbiol.* **2001**, *67*, 539−545.
(48) Tuma, R. S.; Beaudet, M. P.; Jin, X. K.; Jones, L. J.; Cheung, C. Y.; Yue, S.; Singer, V. L. *Anal. Biochem.* **1999**, *268*, 278−288.
(49) Teresa, M.; Gomes, S. R.; Tavares, K. S.; Oliveira, J. *Analyst* **2000**, *125*, 1983−1986.
(50) Zhang, Y.; Tian, J.; Zhai, J.; Luo, Y.; Wang, L.; Li, H.; Sun, X. *J. Fluoresc.* **2011**, *21*, 1841−1846.
(51) Wang, L. H.; Liu, X. F.; Hu, X. F.; Song, S. P.; Fan, C. H. *Chem. Commun.* **2006**, 3780−3782.
(52) Li, T.; Wang, E.; Dong, S. J. *Chem. Commun.* **2009**, 580−582.
(53) Yang, X.; Li, T.; Li, B. L.; Wang, E. K. *Analyst* **2010**, *135*, 71−75.
(54) Walmsley, J. A.; Burnett, J. F. *Biochemistry* **1999**, *38*, 14063−14068.
(55) Xia, W. S.; Schmehl, R. H.; Li, C. J. *J. Am. Chem. Soc.* **1999**, *121*, 5599−5600.
(56) Shi, C.; Gu, H. X.; Ma, C. P. *Anal. Biochem.* **2010**, *400*, 99−102.
(57) Ueyama, H.; Takagi, M.; Takenaka, S. *J. Am. Chem. Soc.* **2002**, *124*, 14286−14287.
(58) Thibon, A.; Pierre, V. C. *J. Am. Chem. Soc.* **2009**, *131*, 434−435.
(59) He, F.; Tang, Y. L.; Wang, S.; Li, Y. L.; Zhu, D. B. *J. Am. Chem. Soc.* **2005**, *127*, 12343−12346.
(60) Radi, A. E.; O'Sullivan, C. K. *Chem. Commun.* **2006**, 3432−3434.